# Structure Determination of SnSb₂S₄ and SnSb₂Se₄ by High-Resolution Electron Microscopy

By Piers P. K. Smith and John B. Parise

*Research School of Chemistry, The Australian National University, GPO Box 4, Canberra, ACT 2601, Australia*

## Abstract

The structure of $SnSb_2Se_4$ has been refined from single-crystal X-ray data, using a starting model obtained from high-resolution transmission electron micrographs of the isostructural sulphide $SnSb_2S_4$. The metal-atom positions are resolved directly in [001] electron microscope images and the anion positions are inferred from related structures. The structure consists of ribbons of edge-sharing semi-octahedra $MX_5$ parallel to $z$; these ribbons are linked by shared S/Se atoms. Crystal data: $SnSb_2S_4$: $M_r = 490.4$, $Pnnm$, $a = 25.641$ (5), $b = 20.381$ (4), $c = 3.8973$ (5) Å, $V = 2037$ Å³, $Z = 12$, $D_x = 4.80$ Mg m⁻³; $SnSb_2Se_4$: $M_r = 678.0$, $Pnnm$, $a = 26.610$ (3), $b = 21.066$ (3), $c = 4.0423$ (5) Å, $V = 2266$ Å³, $Z = 12$, $D_x = 5.96$ Mg m⁻³, Mo $K\alpha$, $\lambda = 0.7107$ Å, $\mu = 29.2$ mm⁻¹, $F(000) = 3456$, $T = 294$ K, $R = 0.045$ for 1687 reflections. (The JCPDS File No. for $SnSb_2S_4$ is 35-1496.)

## Introduction

Studies of the phase equilibria and crystal chemistry of the system Sn–Sb–S have led to contradictory results (Moh, 1975). One reason for this has been the difficulty of obtaining single crystals of the Sn,Sb sulphosalts suitable for X-ray structure determination. As part of a study of the section SnS–Sb₂S₃ Smith (1984) determined the structure of Sn₃Sb₂S₆ by means of high-resolution transmission electron microscopy (HRTEM); the structure model was confirmed by X-ray powder diffraction and subsequently refined by neutron powder diffraction (Parise, Smith & Howard, 1984). In the present paper we report the structure determination of SnSb₂S₄ by HRTEM; single crystals of the sulphide could not be obtained, but a single-crystal X-ray refinement of the Se analogue SnSb₂Se₄ has been carried out in order to confirm the structure model.

A phase of composition SnSb₂S₄ was synthesized by Gaudin & Hamlyn (1938) and Vogel & Gilde (1949), although these authors did not report any diffraction data. Wang & Eppelsheimer (1976) reported a unit cell for a monoclinic phase 'SnSb₂S₄', but a recent structure determination has shown that this phase has the composition Sn₆Sb₁₀S₂₁ (Parise & Smith, 1984). The X-ray powder diffraction patterns for phases of nominal composition SnSb₂S₄ given by Bok & de Wit (1963) and Sachdev & Chang (1975) also correspond closely to that calculated for Sn₆Sb₁₀S₂₁. There is thus no previous substantiated report of the orthorhombic SnSb₂S₄ described in the present paper.

In phase-equilibrium studies of the system SnSe–Sb₂Se₃ Wobst (1968) and Gospodinov, Odin & Novoselova (1975) reported the existence of a phase of composition Sn₂Sb₆Se₁₁. The unit-cell parameters were not determined, but the limited X-ray powder diffraction data given by Gospodinov *et al.* (1975) indicate that this phase corresponds to the phase SnSb₂Se₄ described in the present paper.

## Experimental

### (i) SnSb₂S₄

SnSb₂S₄ was synthesized from the elements combined in stoichiometric proportion in an evacuated silica ampoule. The charge was held at 1073 K for 15 h, then at 743 K for 400 h. Guinier powder X-ray diffraction and electron diffraction revealed the presence of minor Sn₃Sb₂S₆ and Sb₂S₃ in addition to SnSb₂S₄. Approximate unit-cell parameters were determined by electron diffraction; these were subsequently refined from the Guinier data, using the program *LAZY PULVERIX* (Yvon, Jeitschko & Parthé, 1977) to calculate the powder pattern of the TEM-derived structure model in order to index the experimental Guinier pattern; cell refined from 25 reflections, $6.7° < \theta < 27°$, Cu $K\alpha_1$, $\lambda = 1.54056$ Å. Although the sample appears crystalline, Weissenberg photography showed the crystals to be multiple or twinned and a crystal suitable for single-crystal diffractometry could not be found.

Electron microscopy was carried out on a sample prepared from the composition (SnS)₅(Sb₂S₃)₂, 778 K, 576 h. The product contained Sn₃Sb₂S₆ and Sb₂S₃ in addition to SnSb₂S₄. To obtain interpretable structural information from HRTEM images the structure must be imaged along the shortest crystallographic repeat direction; since the material cleaves parallel to the z axis cleavage fragments could not be used for [001] imaging. Thin foils were therefore prepared by ion-beam bombardment and suitably oriented crystals were selected for microscopy.

HRTEM images were obtained with a JEOL 200CX electron microscope equipped with a high-resolution objective-lens pole piece ($C_s = 1\cdot 2$ mm) and a double-tilt goniometer stage ($\pm 10°$), operating at an accelerating voltage of 200 kV. Exposure times were typically 8 s at a magnification of 550 000 times. Images were recorded at approximately the Scherzer defocus ($\Delta f = -1\cdot 2\sqrt{C_s}\lambda = -660$ Å) to give optimum phase contrast (Scherzer, 1949). Under these conditions the image of a sufficiently thin crystal corresponds to the projected charge density (PCD) of the structure, to a resolution limit of approximately $0\cdot 6 \times C_s^{1/4}\lambda^{3/4}$ ($\approx 2\cdot 2$ Å). The limits of applicability of the PCD approximation are discussed by O'Keefe (1973) and Lynch, Moodie & O'Keefe (1975). Fig. 1 shows the [001] HRTEM image of $SnSb_2S_4$.

From the published structures of the chemically related compounds $Sn_4Sb_6S_{13}$ (Jumas, Olivier-Fourcade, Philippot & Maurin, 1980) and $Sn_6Sb_{10}S_{21}$ (Parise & Smith, 1984) we can anticipate that the structure of $SnSb_2S_4$ will contain ribbons of edge-sharing semi-octahedra (pyramids) running parallel to the short crystallographic repeat direction. These ribbons, which correspond to layers of the SnS-type structure ($B16$), have metal–metal distances of approximately $4\cdot 3$ Å (parallel to the ribbon) and $3\cdot 6$ Å (diagonally across the ribbon) when projected along the $\sim 4$ Å axis. These distances are resolved in the HRTEM image, the metal atoms appearing as dark spots in the image of the thinnest part of the crystal. In Fig. 1 the metal positions are indicated in the outlined unit cell and they may be compared with those in the structure drawing (Fig. 2).

The metal positions were thus located directly by HRTEM and the anion positions were then inferred, assuming the structure to consist of $B16$-type ribbons. The heights of the atoms ($z = 0$ or $0\cdot 5$) are fixed by the requirement that the coordination polyhedra around the cations be either single- or double-capped
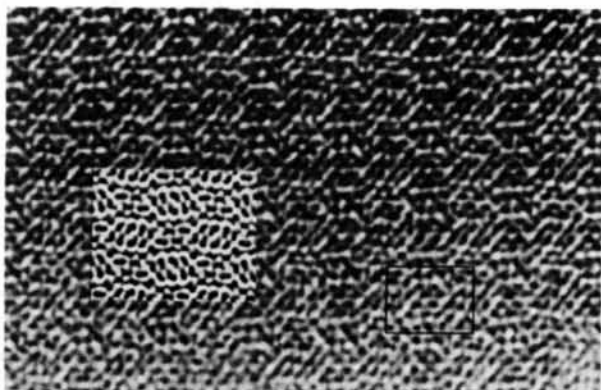
trigonal prisms, as in $Sn_4Sb_6S_{13}$ and $Sn_6Sb_{10}S_{21}$. The resulting structure model (Fig. 2) requires that the phase have the composition $M_3X_4$ and space group $Pnnm$. The symmetry was confirmed by electron diffraction of $SnSb_2S_4$ and by X-ray diffraction of the Se analogue (see below). Peak intensities on the Guinier pattern of $SnSb_2S_4$ were measured with a Joyce–Loebl scanning microdensitometer. The intensities agree well with those calculated assuming the final atomic positions determined for the selenide.[*]

Further confirmation of the structure of $SnSb_2S_4$ is given by the calculated HRTEM image (Fig. 1, inset). The simulated image was computed by means of the multislice method (Cowley & Moodie, 1957; Goodman & Moodie, 1974), using a suite of programs written by Anstis (1983). The multislice is calculated using the algorithm of Ishizuka & Uyeda (1977) and includes 2795 diffracted beams. The best match with the experimental image is obtained with a crystal thickness of 20 Å and an objective-lens defocus of $-575$ Å, although the calculated image changes only slightly for values of the defocus between $-500$ and $-650$ Å. Since the structure model is confirmed by X-ray diffraction we have not attempted to match experimental and computed images for thicker crystals or for other defocus values.

### (ii) $SnSb_2Se_4$

The binary selenides SnSe and $Sb_2Se_3$ are isostructural with the corresponding sulphides, suggesting that the ternary compounds $SnSb_2Se_4$ and $SnSb_2S_4$ may be isostructural. We therefore synthesized $SnSb_2Se_4$ in an attempt to obtain single crystals for X-ray diffractometry. Evacuated silica ampoule; Sn, Sb and Se in stoichiometric ratio; 1123 K for 4 h then 813 K for 120 h. The Guinier pattern of the product was indexed assuming the structure model derived
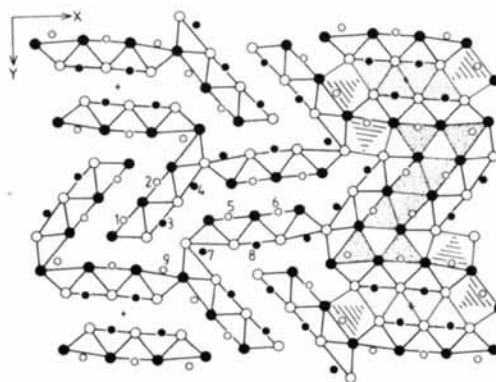
[*] See deposition footnote.



Fig. 1. [001] HRTEM image of $SnSb_2S_4$. The unit cell ($25\cdot 6 \times 20.4$ Å) is outlined at lower right with the 36 metal-atom sites indicated by dots; cf. Fig. 2. The inset (left) is a computed image assuming the structure refined for $SnSb_2Se_4$.



Fig. 2. The structure of $SnSb_2Se_4$ and $SnSb_2S_4$ projected on (001); coordinates from the selenide refinement. Small circles Sn/Sb, large circles S/Se; open circles $z = 0$, filled circles $z = 0\cdot 5$.

Table 1. *Final atom parameters* $(\times 10^4)$ *for* $SnSb_2Se_4$; *e.s.d.'s* $1 \times 10^{-4}$ *for positional parameters and* $5 \times 10^{-4}$ *for thermal parameters; e.s.d.'s for* $U_{eq}$ *estimated according to the recommendations of Schomaker & Marsh* (1983)

$$U_{eq} = \tfrac{1}{3}(U_{11} + U_{22} + U_{33}).$$

| | $x$ | $y$ | $z$ | $U_{eq}(\text{Å}^2)$ |
|---|---|---|---|---|
| $M(1)^*$ | 86 | 5903 | 0 | 203 |
| $M(2)$ | 1265 | 4256 | 0 | 283 |
| $M(3)$ | 1434 | 6057 | $\frac{1}{2}$ | 278 |
| $M(4)$ | 2549 | 4485 | $\frac{1}{2}$ | 394 |
| $M(5)$ | 3702 | 5852 | 0 | 199 |
| $M(6)$ | 5432 | 5678 | 0 | 218 |
| $M(7)$ | 2785 | 7359 | $\frac{1}{2}$ | 471 |
| $M(8)$ | 4647 | 7105 | $\frac{1}{2}$ | 286 |
| $M(9)$ | 1406 | 8134 | 0 | 340 |
| Se(1) | 9671 | 6579 | $\frac{1}{2}$ | 204 |
| Se(2) | 769 | 5119 | $\frac{1}{2}$ | 167 |
| Se(3) | 1787 | 3612 | $\frac{1}{2}$ | 173 |
| Se(4) | 872 | 6655 | 0 | 164 |
| Se(5) | 1969 | 5138 | 0 | 168 |
| Se(6) | 2913 | 3477 | 0 | 161 |
| Se(7) | 3021 | 5977 | $\frac{1}{2}$ | 160 |
| Se(8) | 4610 | 5834 | $\frac{1}{2}$ | 158 |
| Se(9) | 6158 | 5607 | $\frac{1}{2}$ | 145 |
| Se(10) | 2206 | 6961 | 0 | 178 |
| Se(11) | 3865 | 7065 | 0 | 160 |
| Se(12) | 5488 | 6904 | 0 | 158 |

* (Sn,Sb) distributed randomly over the nine available metal (M) sites.

Table 2. *Selected interatomic distances* (Å) *for* $SnSb_2Se_4$

| | | | |
|---|---|---|---|
| $M(1)$–Se(4) | 2·624 (3) | $M(6)$–Se(12) | 2·587 (3) |
| –Se(1) ×2 | 2·708 (2) | –Se(9) ×2 | 2·800 (2) |
| –Se(2) ×2 | 3·181 (2) | –Se(8) ×2 | 2·996 (2) |
| –Se(2) ×2 | 3·728 (3) | –Se(8) ×2 | 3·774 (2) |
| $M(2)$–Se(5) | 2·638 (3) | $M(7)$–Se(10) ×2 | 2·676 (3) |
| –Se(3) ×2 | 2·803 (2) | –Se(7) | 2·978 (2) |
| –Se(2) ×2 | 3·022 (2) | –Se(6) | 2·999 (2) |
| –Se(1) ×2 | 3·658 (3) | –Se(3) ×2 | 3·514 (2) |
| | | –Se(11) ×2 | 3·568 (2) |
| $M(3)$–Se(2) | 2·653 (3) | | |
| –Se(4) ×2 | 2·812 (2) | $M(8)$–Se(8) | 2·677 (3) |
| –Se(5) ×2 | 3·140 (2) | –Se(11) ×2 | 2·902 (2) |
| –Se(10) ×2 | 3·454 (2) | –Se(12) ×2 | 3·045 (2) |
| | | –Se(1) ×2 | 3·433 (2) |
| $M(4)$–Se(3) | 2·737 (3) | | |
| –Se(5) ×2 | 2·891 (2) | $M(9)$–Se(9) | 2·733 (3) |
| –Se(6) ×2 | 3·087 (2) | –Se(6) ×2 | 2·809 (2) |
| –Se(7) | 3·385 (2) | –Se(12) ×2 | 3·172 (2) |
| –Se(9) | 3·446 (2) | –Se(10) | 3·262 (3) |
| | | –Se(4) | 3·424 (3) |
| $M(5)$–Se(11) | 2·592 (3) | | |
| –Se(7) ×2 | 2·727 (2) | | |
| –Se(8) ×2 | 3·150 (2) | | |
| –Se(9) ×2 | 3·697 (2) | | |

for the sulphide. The cell parameters were refined from the Guinier data (Cu $K\alpha_1$, $\lambda = 1\cdot54056$ Å, 24 reflections, $13° < \theta < 28°$).

Weissenberg and precession photographs confirmed the assignment of space group *Pnnm* and were used to check the quality of the crystal (needle-shaped fragment $0\cdot05 \times 0\cdot02 \times 0\cdot26$ mm) selected for data collection. Philips PW 1100 diffractometer. 2917 reflections measured in the range $2° < 2\theta < 50°$, $(\sin \theta / \lambda)_{max} = 0\cdot6$ Å$^{-1}$. Following corrections for Lorentz factor, polarization and absorption ($\bar{T}_{max} = 0\cdot54$, $\bar{T}_{min} = 0\cdot27$) symmetry-equivalent reflections were averaged to yield 2108 unique data with $F_{obs} > 0\cdot0$. Of these, 421 with $F_{obs} < 2\sigma(F_{obs})$ were excluded from the refinement. $R_{int}$ (Sheldrick, 1976) from merging equivalent reflections was $0\cdot044$.

The structure derived from the HRTEM images of $SnSb_2S_4$ was used as a starting point for the least-squares refinement. Initial isotropic refinement confirmed the model to be correct and the final calculation assuming anisotropic thermal motion for all atoms converged on the discrepancy indices $R = 0\cdot045$ and $R_w = 0\cdot036$. The individual reflection weights were $[\sigma^{-2}(F_{obs})]$. In the final cycle $(\Delta/\sigma)_{max} = 0\cdot1$. The final atomic parameters are given in Table 1.*

---

* Lists of structure factors and anisotropic thermal parameters for $SnSb_2Se_4$, together with powder diffraction data for $SnSb_2S_4$, have been deposited with the British Library Lending Division as Supplementary Publication No. SUP 39569 (14 pp.). Copies may be obtained through The Executive Secretary, International Union of Crystallography, 5 Abbey Square, Chester CH1 2HU, England.

The maximum and minimum values in the final difference Fourier map were 2·2 and $-2\cdot6$ e Å$^{-3}$. These features were close to the metal positions, indicating slight inadequacies in either the disordered Sn,Sb distribution over the nine available metal sites, the modelling of thermal motion, or the absorption correction. An ordered arrangement of Sn and Sb based on the distribution of peaks in the difference map failed to improve the overall fit of the model to the observed data. Similarly, small changes in the values used for the crystal size failed to improve the overall fit significantly. The difficulty in measuring the two smallest dimensions of the crystal results in uncertainty in the absorption correction.

Analytical expressions for the scattering factors were taken from *International Tables for X-ray Crystallography* (1974). Calculations were carried out on the Australian National University Univac 1100/82 computer; programs used were *SHELX*76 (Sheldrick, 1976) and *ORTEP* (Johnson, 1965).

**Discussion**

Fig. 2 shows the final structure of $SnSb_2Se_4$ projected on (001); bond lengths are given in Table 2. As assumed in deriving the structure, it is built from ribbons of edge-sharing semi-octahedra that extend along z. These ribbons are hinged together by sharing of Se atoms between adjacent ribbons. Within each ribbon the cations are offset from the centre of the pyramid base, giving [1 + 2 + 2] coordination; the ribbons are thus very similar to the infinite sheets of the SnS structure (Wiedemeier & von Schnering, 1978).

With the exception of $M(7)$, the shortest bond is that between the cation and the summit of the pyramid.

The right-hand part of Fig. 2 shows how the juxtaposition of these basic structural units gives rise to trigonal-prismatic coordination of all the cations by Se, the prisms being represented by dot shading (prism axis parallel to $z$) or line shading [prism axis in (001)]. For all cations except $M(7)$ the prism has a single cap formed by the short $M$-Se bond of the pyramid summit. Fig. 3 shows a typical example, the coordination polyhedron of $M(1)$. Notice that for $M(4)$ and $M(9)$ the monocapped prism has its axis in (001).

Cation $M(7)$ is shared between two hinged ribbons and it consequently lies in a bicapped trigonal prism of Se atoms (Fig. 4). Unlike the other metal atoms, which lie close to the basal plane of the pyramidal cap, $M(7)$ lies aproximately on the bisector of the acute angle between the two articulated ribbons. The shortest $M$-Se distances for $M(7)$ are thus the two equivalent distances to the shared Se(10), rather than to the capping Se atoms. It is interesting to note that $M(7)$ has the largest and most anisotropic thermal parameter of all the metal atoms, with the principal vibration direction along a line joining the two prism caps Se(6) and Se(7). $M(7)$ is thus directly analogous to $M(6)$ of $Sn_4Sb_6S_{13}$ (Jumas et al., 1980) and $M(14)$ of $Sn_6Sb_{10}S_{21}$ (Parise & Smith, 1984) which also lie in bicapped prisms and have elevated anisotropic thermal parameters. In all three structures this situation arises where the metal atom is shared between two hinged ribbons.
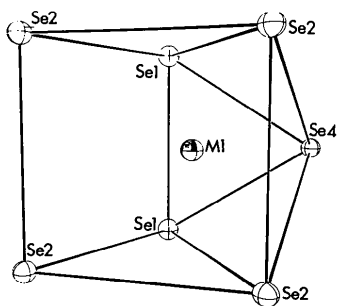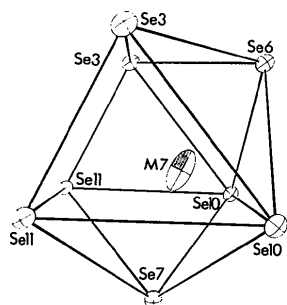
The structure refinement of $SnSb_2Se_4$ confirms the structure model derived for $SnSb_2S_4$ by HRTEM. It is clear from this and from the powder diffraction and electron diffraction data that the two compounds are isostructural, although only the selenide structure has been refined. The final atomic parameters for the selenide are very close to those of the initial model, with a mean displacement from the original positions of 0·40 Å for the cations and 0·21 Å for the anions. The accuracy in the initial model is greater than could be obtained from HRTEM alone and depends on information concerning related structures in the system $SnS$-$Sb_2S_3$, particularly for the location of the anions. However, HRTEM has now been used to determine the initial structure model for $Sn_3Sb_2S_6$ (Smith, 1984) and $SnSb_2S_4$ and is clearly a powerful method for solving structures in cases where single crystals cannot be grown and where there is a suitable short projection axis.

Fig. 3. Coordination polyhedron of $M(1)$.



Fig. 4. Coordination polyhedron of $M(7)$.

**References**

ANSTIS, G. R. (1983). *Multislice Program Package*. Research School of Chemistry, Australian National Univ.

BOK, L. D. C. & DE WIT, J. H. (1963). *Z. Anorg. Allg. Chem.* **324**, 162–167.

COWLEY, J. M. & MOODIE, A. F. (1957). *Acta Cryst.* **10**, 609–619.

GAUDIN, A. M. & HAMLYN, W. T. (1938). *Econ. Geol.* **33**, 868–888.

GOODMAN, P. & MOODIE, A. F. (1974). *Acta Cryst.* **A30**, 280–290.

GOSPODINOV, G. G., ODIN, I. N. & NOVOSELOVA, A. F. (1975). *Inorg. Mater.* (*USSR*), **11**, 1033–1035.

*International Tables for X-ray Crystallography* (1974). Vol. IV. Birmingham: Kynoch Press.

ISHIZUKA, K. & UYEDA, N. (1977). *Acta Cryst.* **A33**, 740–749.

JOHNSON, C. K. (1965). *ORTEP*. Report ORNL-3794. Oak Ridge National Laboratory, Tennessee.

JUMAS, J. C., OLIVIER-FOURCADE, J., PHILIPPOT, E. & MAURIN, M. (1980). *Acta Cryst.* **B36**, 2940–2945.

LYNCH, D. F., MOODIE, A. F. & O'KEEFE, M. A. (1975). *Acta Cryst.* **A31**, 300–307.

MOH, G. H. (1975). *Chem. Erde*, **34**, 201–238.

O'KEEFE, M. A. (1973). *Acta Cryst.* **A29**, 389–401.

PARISE, J. B. & SMITH, P. P. K. (1984). *Acta Cryst.* **C40**, 1772–1776.

PARISE, J. B., SMITH, P. P. K. & HOWARD, C. J. (1984). *Mater. Res. Bull.* **19**, 503–508.

SACHDEV, S. C. & CHANG, L. L. Y. (1975). *Econ. Geol.* **70**, 1111–1122.

SCHERZER, O. (1949). *J. Appl. Phys.* **20**, 20–29.

SCHOMAKER, V. & MARSH, R. E. (1983). *Acta Cryst.* **A39**, 819–820.

SHELDRICK, G. M. (1976). *SHELX76*. A program for crystal structure determination. Cambridge Univ.

SMITH, P. P. K. (1984). *Acta Cryst.* **C40**, 581–584.

VOGEL, R. & GILDE, W. (1949). *Z. Metallkd.* **40**, 121–126.

WANG, N. & EPPELSHEIMER, D. (1976). *Chem. Erde*, **35**, 179–184.

WIEDEMEIER, H. & VON SCHNERING, H. G. (1978). *Z. Kristallogr.* **148**, 295–303.

WOBST, M. (1968). *J. Less-Common Met.* **14**, 77–81.

YVON, K., JEITSCHKO, W. & PARTHÉ, E. (1977). *J. Appl. Cryst.* **10**, 73–74.